

# Charge Transfer during the Aluminum–Water Reaction Studied with Schottky Nanodiode Sensors

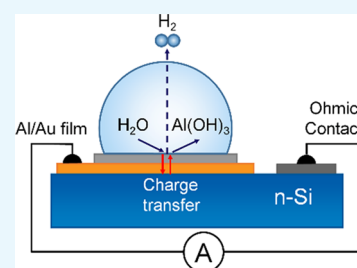
Ievgen I. Nedrygailov,<sup>†,#</sup> Yeob Heo,<sup>†,‡</sup> Heeyoung Kim,<sup>†,‡</sup> and Jeong Young Park<sup>\*,†,‡</sup>

<sup>†</sup>Center for Nanomaterials and Chemical Reactions, Institute for Basic Science, Daejeon 34141, Republic of Korea

<sup>‡</sup>Department of Chemistry and EEWS Graduate School, Korea Advanced Institute of Science and Technology (KAIST), Daejeon 34141, Republic of Korea

## Supporting Information

**ABSTRACT:** The aluminum–water reaction is a promising source for hydrogen production. However, experimental studies of this reaction are difficult because of the highly concentrated alkaline solution used to activate the surface of aluminum. Here, we show that the reaction kinetics can be monitored in real time by a Schottky diode sensor, consisting of an ultrathin aluminum film deposited on a semiconductor substrate. Charge resulting from the corrosion of the aluminum film causes an electrical signal in the sensor, which is proportional to the rate of the chemical process. We discuss the possible mechanisms for the reaction-induced charge generation and transfer, as well as the use of Schottky diode based sensors for operando studies of the aluminum–water reaction and similar reactions on metals in concentrated alkaline solutions.



## 1. INTRODUCTION

In recent years, the study of hydrogen generation from chemical reactions of metal particles with water has become increasingly relevant.<sup>1–3</sup> One such reaction, often considered as a potential source of inexpensive hydrogen for mobile energy sources, is the reaction of aluminum and water (i.e.,  $\text{Al} + 3\text{H}_2\text{O} \rightarrow \text{Al}(\text{OH})_3 + 3/2\text{H}_2$ ).<sup>4–7</sup> The main advantages of aluminum as a source of hydrogen are high activity, storage safety, ease of transportation, and renewability.<sup>8,9</sup> Under normal conditions, the rate of Al–water reaction is quite low because the aluminum surface is covered with a thin oxide film that forms a so-called “barrier layer” that prevents the interaction of  $\text{H}_2\text{O}$  molecules with the Al surface.<sup>4</sup> Thus, the Al–water reaction only occurs in the presence of extremely caustic substances, such as NaOH and KOH, which dissolve the oxide film and activate the Al surface to interact with water molecules. Since the caustic base is not consumed in the reaction, it can be considered as a catalyst for this process. Also, a number of studies based on ab initio molecular dynamics simulations show that the chemical reactivity of Al changes drastically in the transition from microscopic particles to nanoparticles and clusters.<sup>3,10–12</sup> Combining the results of these studies with experimental data would be a significant step forward in engineering technology for hydrogen production based on the Al–water reaction.

Given the nature of the Al–water reaction, studies of the reaction mechanism can be carried out using conventional methods. Among them are electrochemical methods that are simultaneously simple and powerful.<sup>13</sup> However, despite the advantages of this technique, its application is possible only under the conditions of the applied electric potential, which can lead to irreversible changes in the studied medium (e.g., parallel electrochemical processes may be triggered and form

various by-products not related to the test reaction, thus complicating the interpretation of experimental data). In addition, electrochemical methods limit observation to the overall reaction occurring in the reaction cell while making it impossible to see certain stages of the reaction isolated from processes occurring on other electrodes. Therefore, the development of new, noninvasive experimental methods, in addition to those existing for operando studies of the Al–water reaction under realistic reaction conditions, gains special attention.

In this paper, we consider the effects of charge transfer on the surfaces of ultrathin Al films in concentrated NaOH solutions under reaction conditions and discuss the possible use of these effects for operando studies of the Al–water reaction. We show that the reaction-induced generation and transfer of electrical charge on the Al surface can be monitored by a Schottky nanodiode sensor based on a metal–semiconductor contact. The principle of operation of the sensor is illustrated in Figure 1a. An ultrathin metal film is placed on the surface of a semiconductor substrate so that it creates a Schottky contact. At equilibrium, the electrical current through the metal–semiconductor contact is zero because the thermionic emission current flowing through the Schottky contact in the forward and reverse directions is balanced.<sup>14,15</sup> However, when a chemical reaction proceeds on the metal surface, the equilibrium can be disturbed by the formation of excess charge, which leads to the appearance of a nonzero electrical current.<sup>15–20</sup> A number of research papers show that this current is proportional to the reaction rate, which makes

Received: October 12, 2019

Accepted: November 15, 2019

Published: November 27, 2019

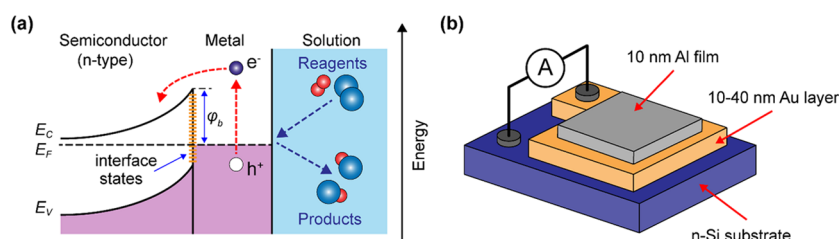


**Figure 1.** (a) Principle of operation of a Schottky nanodiode sensor based on a metal–semiconductor contact. (b) Schematics of the sensor consisting of an ultrathin Al film deposited onto the surface of a planar Au/n-Si Schottky nanodiode.

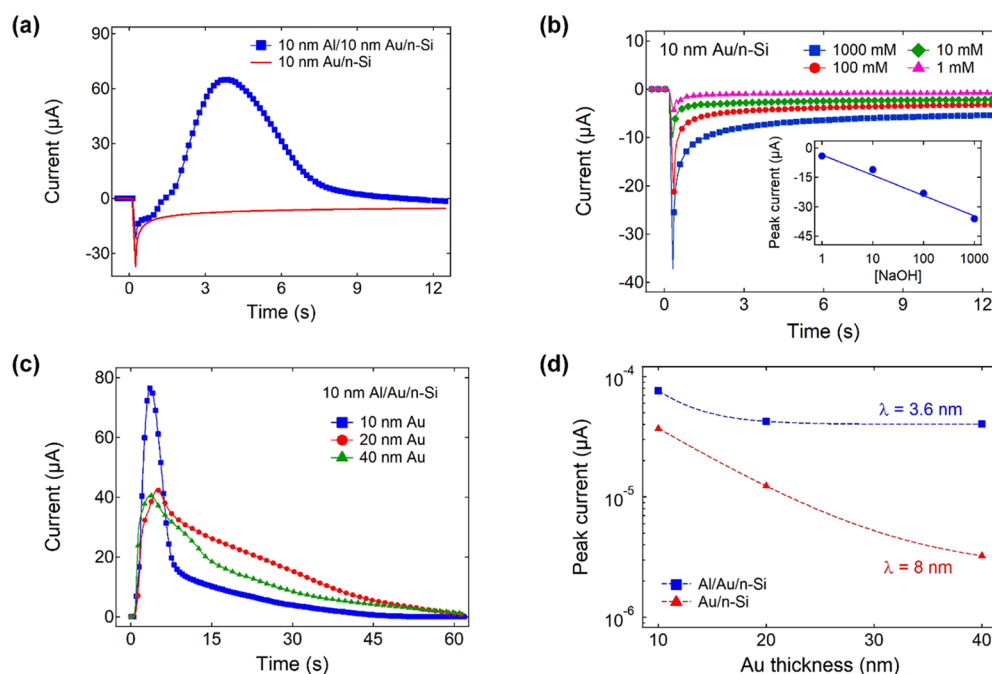


**Figure 2.** (a) Typical response of the 10 nm Al/10 nm Au/n-Si and 10 nm Au/n-Si nanodiode sensors immersed in concentrated NaOH solutions. (b) Initial peaks measured from the 10 nm Au/n-Si nanodiode sensor in a concentrated NaOH solution. (c) Reaction currents measured by the Al/Au/n-Si nanodiode sensor with Au layer thicknesses varying from 10 to 40 nm. (d) Magnitude of the initial peak and reaction current with varying thicknesses of the Au layer.

nanodiode sensors a convenient tool for studying chemical kinetics on nanoscale metal structures.<sup>21–25</sup> We may also note that various sensors based on Schottky diodes operating by the above mechanism or other mechanisms have been reported for a number of applications in both gas–metal and in liquid–metal reactions.<sup>16,26–31</sup>

## 2. RESULTS AND DISCUSSION

A schematic cross section of a Schottky nanodiode sensor is shown in Figure 1b. To ensure reliable electrical contact with the sensor under the Al corrosion conditions during its reaction with water, a thin layer of Au was applied between the Al film and the semiconductor substrate. Thus, the sensor is a three-layer structure: a chemically active Al film on top, a Au layer in the middle, and a semiconductor substrate at the bottom. A typical response of the 10 nm Al/10 nm Au/n-Si nanodiode sensor to the Al–water reaction in a concentrated NaOH solution is shown in Figure 2a. At the moment when the sensor first comes into contact with the solution, a sharp current peak is observed (hereafter referred to as the initial peak) that disappears after a few seconds. The polarity of the initial peak corresponds to the transfer of an electron from the metal to the semiconductor (i.e., it is a reverse (negative)

current through the Schottky contact). It is important to note that a similar initial peak is also observed when the concentrated NaOH solution interacts with 10 nm Au/n-Si nanodiode sensors. It is obvious that, in this case, the chemical reaction does not occur on the sensor surface due to the absence of aluminum. Thus, we presume that the initial peak is caused by the charging of the sensor surface via adsorption of ions from the NaOH solution. The double layer formed during this process most likely causes electric charge redistribution at the metal–semiconductor contact, which leads to the appearance of the initial peak. For further analysis, the initial peak as a function of the NaOH concentration in the solution was measured with a 10 nm Au/n-Si nanodiode sensor. As shown in Figure 2b, the magnitude of the initial peak increases as the NaOH concentration in the solution increases. This confirms the hypothesis about the relationship between this current signal and the accumulation of charge on the sensor surface.

After the initial peak, another type of current signal can be detected. This signal, hereafter referred to as the reaction current, flows in the forward (positive) direction and corresponds to electron transfer from the semiconductor to the metal. When the reaction current occurs, gas bubbles

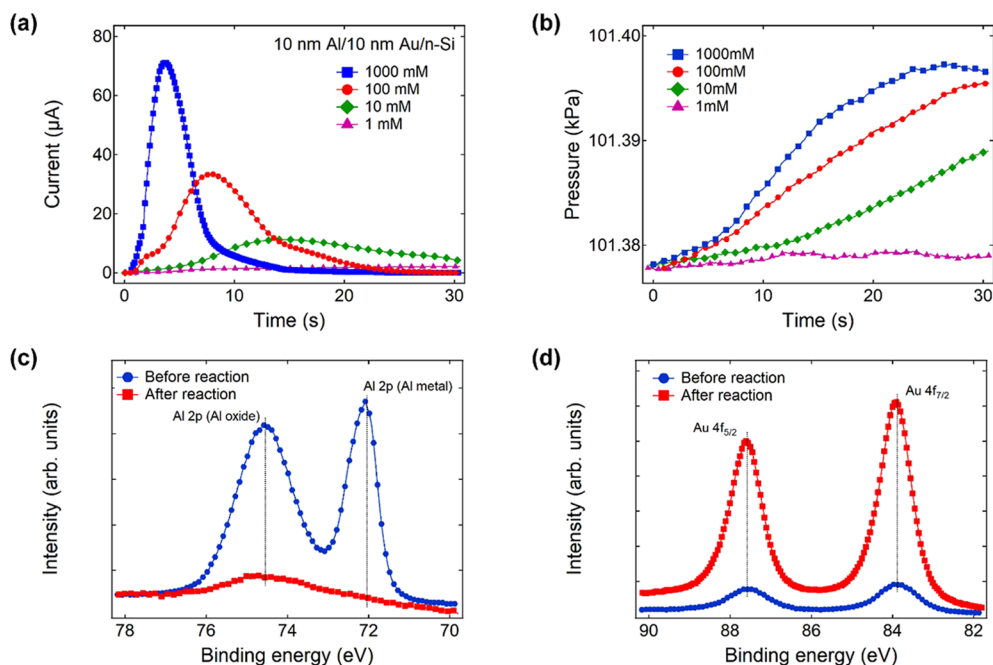


**Figure 3.** (a) Response of the 10 nm Al/10 nm Au/n-Si nanodiode sensor and (b) corresponding changes in total pressure in the reactor during the Al–water reaction in a concentrated NaOH solution. (c,d) High-resolution XPS spectra of the Al 2p and Au 4f peaks, measured from the 10 nm Al/10 nm Au/n-Si nanodiode sensor before and after the Al–water reaction in a 1000 mM NaOH solution.

appear on the sensor surface. The amount of gas generated on the sensor with the 10 nm thick Al film is too small to analyze its composition. However, a mass spectrometric study of the gas generated in the Al–water reaction, carried out in a separate experiment with thicker Al films and foils, indicates that the generated gas is hydrogen (see Figure S2). Thus, we can conclude that the appearance of bubbles on the sensor surface indicates the onset of  $\text{H}_2$  evolution during the Al–water reaction. The reaction current is only observed on the nanodiode sensors with an Al film, and its magnitude shows a clear correlation with the reaction rate, which can be determined from the rate of gas evolution. Thus, we can conclude that the reaction current is a consequence of the Al–water reaction. Based on this, and also for the sake of simplicity in the following figures, we only show data related to the reaction current, which is determined by subtracting the current signals measured on nanodiode sensors with and without an Al film in the same solution.

Figure 2c shows the reaction current measured by the Al/Au/n-Si nanodiode sensors with the thickness of the Au layer varying from 10 to 40 nm. The thickness of the Al film was 10 nm for all the experiments. As can be seen, the reaction current shows a clear dependence on the thickness of the Au layer. This effect clearly indicates the nonthermal nature of the reaction current.<sup>15,22</sup> Thus, we can state that the current observed in the nanodiode sensors during the Al–water reaction does not result from the thermoelectric effect caused by surface heating during the reaction. It can also be assumed that the presence of an explicit dependence of the reaction current on the metal thickness may indicate the participation of hot electrons in the current generation process. The occurrence of the reaction current, called a chemi-current, due to the transfer of hot electrons in Schottky nanodiodes is well known for exothermic reactions at both gas–metal<sup>21,22,32</sup> and liquid–metal interfaces.<sup>29,33</sup> Because of the scattering processes that occur when moving through a metal film, a

current of hot electrons usually demonstrates a strong dependence on the thickness of the metal electrodes in nanodiode sensors.<sup>21,22</sup> Thus, a similar process can be expected for the Al–water reaction at the surface of the Al/Au/n-Si nanodiode sensors. It is interesting to note that the dependence of the current on the thickness of the metal film is also observed for the initial peak (see Figure 2d). Both the initial peak and the reaction current can be described by the exponential function  $I = I_0 \exp(-d/\lambda)$  when plotted as a function of the Au layer thickness, which is denoted as  $d$ . In Figure 2d, the fitting curves are shown by the dashed lines. The attenuation length  $\lambda$  for the Au/n-Si nanodiode sensors is two times larger than that for the Al/Au/n-Si nanodiode sensors. This fact can be explained within the framework of the hot electron transfer hypothesis by the more complex structure of the metal–semiconductor interface in the Al/Au/n-Si nanodiode sensors, which provides stronger scattering of the hot electron flux.

In the most concentrated alkaline solution ( $[\text{NaOH}] = 1000$  mM), the reaction current reaches a significant peak value of  $70 \mu\text{A}$ , just a few seconds after the start of the experiment. As the concentration of the solution decreases, the magnitude of the reaction current decreases as well. In this case, the peak current is observed somewhat later (Figure 3a). Rapid corrosion on the surface of the Al film leads to the fact that the reaction current decreases rapidly and reaches zero in less than a minute after the start of the experiment. By this time, gas evolution from the surface also ceases, as can be seen from the pressure measurements (Figure 3b). In addition, after the completion of the reaction, the Al film completely dissolves, which is clearly visible to the naked eye due to the color change of the active surface of the nanodiode sensor. The dissolution of the Al film is also confirmed by ex situ XPS analysis (Figure 3c,d). SEM images of the surface of the Al/Au/n-Si nanodiode sensor before and after the Al–water reaction are shown in Figure S3.

The data shown in Figure 3a,b allow us to analyze the efficiency of the reaction current generated during the Al–water reaction. In particular, the reaction current yield can be obtained, which is defined as the number of charge carriers detected per H<sub>2</sub> molecule

$$\text{yield} = \frac{N_e}{N_{\text{H}_2}} \times 100 \quad (1)$$

The number of charge carriers ( $N_e$ ) can be estimated by integrating the electrical signal from the sensor over time (i.e.,  $N_e = (1/e) \cdot \int_0^t I dt$ ). In turn, the number of H<sub>2</sub> molecules ( $N_{\text{H}_2}$ ) produced on the sensor can be determined from the change in pressure in the reactor using the ideal gas equation. The yield as a function of NaOH concentration, calculated using eq 1, is shown in Figure 4. As can be seen, the yield is

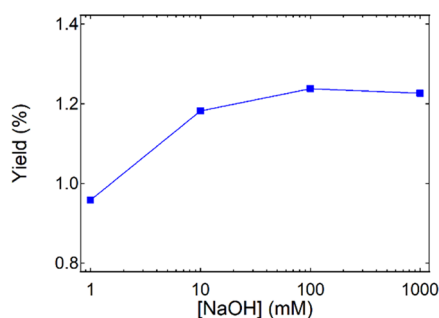
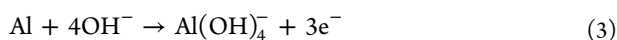
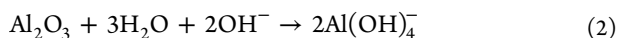


**Figure 4.** Reaction current yield as a function of NaOH concentration derived for the 10 nm Al/10 nm Au/n-Si nanodiode sensor.

around 1% and remains almost unchanged over the whole range of NaOH concentrations. This makes it convenient to use sensors based on Schottky nanodiodes for kinetic studies of the Al–water reaction and other similar reactions at the metal–liquid interface. These findings may have potential applications in novel operando sensing of chemical reactions and can also be useful in the context of recent studies on the electronic control of chemical reactions.<sup>32,34</sup>

The idea of creating a sensor based on a Schottky nanodiode to study charge transfer reactions at the liquid–solid interface was discussed earlier.<sup>35,36</sup> Nevertheless, the number of experimental studies using such sensors is still quite small.<sup>29,37</sup> As far as we know, the present paper is the first to report the detection of electrical signals in metal–semiconductor nanodiode sensors during the Al–water reaction. The nature of this phenomenon is not yet clear. However, based on the reaction mechanism considered elsewhere,<sup>4,13</sup> one could assume the following sequence of events: first, the surface oxide layer is destroyed via interaction with the NaOH solution (reaction 2). Then, as follows from reaction 3, the Al surface interacts with hydroxide ions to form aluminate. The electrons produced by this reaction are consumed by the water reduction reaction (reaction 4). During the water reduction reaction, hydrogen gas is released from the Al surface.



As can be seen in these equations, the Al–water reaction takes place through an anodic (reaction 3) and a cathodic (reaction 4) reaction. Thus, we can consider the path of electrons during the reaction as follows. The electrons produced by the anodic reaction can be consumed by partial cathodic reactions, such as the oxygen reduction reaction and/or water reduction reaction.<sup>13</sup> However, considering the thinness of the Al/Au metal film and the high mobility of electrons, it can also be expected that a fraction of these electrons pass through the metal film and reach the Schottky contact at the Au/Si interface (Figure 5a). As shown

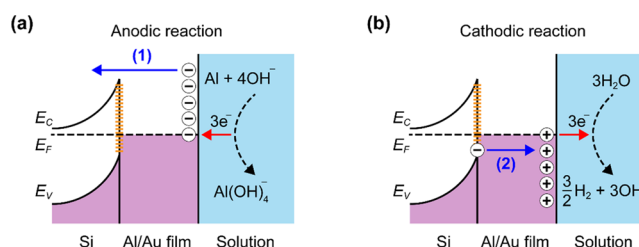


**Figure 5.** Proposed mechanism for the generation of current in the Al/Au/n-Si nanodiode sensor during the Al–water reaction. Here, the redistribution of charge in the sensor is shown for the (a) anodic and (b) cathodic reaction cases.

elsewhere,<sup>21</sup> mobile electrons arising in metal films during an exothermic reaction are carriers of excess energy, which is on the order of 1 eV. Thus, it can be anticipated that electrons resulting from the Al–water reaction are able to overcome the Schottky barrier and enter the semiconductor. This process exceeds the thermionic emission given by eq 5 (see Materials and Methods), and thus, it can be considered as emission of hot electrons across the metal–semiconductor interface. The resulting current may be responsible for the appearance of the initial peak seen in Figure 2a,b. Arguing in a similar way, one can assume that the reaction current (Figure 2a,c) is a consequence of charge transfer from the Schottky barrier region to the near-surface region of the nanodiode sensor. Indeed, the consumption of electrons during the cathodic reaction leads to the depletion of the surface region of the metal film and the formation of holes (Figure 5b). Given the exothermic nature of the Al–water reaction, it can be expected that these holes are formed slightly below the Fermi level in the metal. Examples of a similar process in gas–solid reactions are well known.<sup>21,22,38–44</sup> The current in this case is a consequence of the movement of holes toward the Schottky contact and their neutralization there by electrons from interfacial donor states.<sup>45</sup>

As shown elsewhere,<sup>46</sup> a major fraction of hot electrons created in metal films from the release of chemical energy carry excess energy, which only slightly ( $E - E_F \leq 0.4$  eV) exceeds the Fermi level. Such electrons are not able to overcome the Schottky barrier, which for the case of the Al/Au/n-Si nanodiode sensors reaches  $\phi_b = 0.74$  eV. This causes the small amplitude and duration of the initial peak to be attributed to the anodic reaction. At the same time, the proposed mechanism of charge transfer does not require direct crossing of the Schottky contact by hot holes created during the cathodic reaction. As shown in Figure 5b, in this case, the current flow is compensated for by the transition of electrons through the Schottky barrier in the forward direction, which greatly facilitates the charge transfer process. This could

explain the significantly larger magnitude and duration of the reaction current than the initial peak.

### 3. CONCLUSIONS

We have considered the possibility of using nanodiode sensors based on a Schottky metal–semiconductor contact to study charge transfer effects on the surface of ultrathin Al films in concentrated NaOH solutions under reaction conditions. Electrons arising in the Al film during the anodic reaction of aluminate formation and holes created during the cathodic reduction of water lead to the transfer of excited charge carriers through a Schottky contact in the nanodiode sensor. These processes generate electrical current in the sensor that carries information about surface chemical processes in real time. The current yield of the nanodiode sensor is on the order of 1% and remains constant over the whole range of NaOH concentrations, which makes it convenient to use sensors of this type for operando studies of the Al–water reaction.

### 4. MATERIALS AND METHODS

The sensor was fabricated by vacuum deposition of the metal contacts onto an n-type Si (100) substrate ( $\rho = 1\text{--}10\ \Omega\cdot\text{cm}$ ). Metal evaporation was carried out using several stainless-steel masks with windows of different sizes and shapes that made it possible to simultaneously produce 28 nanodiode sensors with identical properties on a single Si substrate. First, to remove the native oxide, the Si substrate was etched in a buffered oxide solution composed of  $\text{NH}_4\text{F}$  and HF in water for 60 s at room temperature. The Si substrate was then moved to the evaporator chamber for depositing the metal contacts. The Au film (Schottky contact) was deposited onto the polished surface of the Si substrate using electron-beam evaporation at a base pressure of  $2 \times 10^{-6}$  torr and an average deposition rate of  $0.7\ \text{\AA}/\text{s}$ . The total area of the Schottky contact for a single nanodiode sensor was  $A = 116\ \text{mm}^2$ . In the next stage, the nanodiode sensor was supplemented by an ohmic contact. For this, a 50 nm thick Ti film followed by 50 nm of Au was evaporated so that a  $4 \times 7\ \text{mm}^2$  ohmic contact was formed near each Schottky contact. In the final stage, a 10 nm thick Al film with an area of  $10 \times 8\ \text{mm}^2$  was deposited directly onto the Au surface of the Au/n-Si nanodiode.

To obtain the properties of the Schottky barrier at the metal–semiconductor contact of the Al/Au/n-Si nanodiode sensor, current–voltage ( $I$ – $V$ ) curves were measured (see Figure S1). Based on the thermionic emission theory of charge transport, the  $I$ – $V$  curves for a forward-biased Schottky diode are given by

$$I = AA^*T^2 \exp\left(-\frac{e\phi_b}{k_B T}\right) \exp\left(\frac{e(V - IR_{\text{ser}})}{\eta k_B T}\right) \quad (5)$$

where  $A$  is the area of the Schottky contact,  $A^*$  is the Richardson constant,  $T$  is the temperature,  $e$  is the elementary charge,  $\phi_b$  is the Schottky barrier height,  $k_B$  is the Boltzmann constant,  $V$  is the voltage,  $R_{\text{ser}}$  is the series resistance, and  $\eta$  is the ideality factor. The Schottky barrier height obtained by fitting eq 5 to the experimental data is  $\phi_b = 0.74\ \text{eV}$  (at  $\eta = 1.03$  and  $R_{\text{ser}} = 55\ \Omega$ ). This value is somewhat lower than the typical Schottky barrier height  $\phi_b = 0.8\text{--}0.83\ \text{eV}$  reported in the literature for the contact between Au and n-type Si.<sup>14,47</sup> The low Schottky barrier height is explained by the fact that eq 5 does not take into account tunneling effects through defects

and Au-induced gap states at the Au/n-Si interface or the Schottky barrier lowering resulting from image charge.<sup>48</sup>

The apparatus for measuring the current during the Al–water reaction on the surface of the Al/Au/n-Si nanodiode sensor is explained in detail elsewhere.<sup>33</sup> The sample cell containing the NaOH solution was connected to a manipulator that allowed for immersion of the nanodiode sensor into the solution. The current was measured using a model 2400 series SourceMeter from Keithley Instruments, Inc. The rate of Al–water reaction was determined by measuring the amount of  $\text{H}_2$  produced during the reaction where the pressure change as a function of time was measured using a 120AA Baratron high-accuracy absolute-capacitance manometer from MKS Instruments.

### ■ ASSOCIATED CONTENT

#### Supporting Information

The Supporting Information is available free of charge at <https://pubs.acs.org/doi/10.1021/acsomega.9b03397>.

Current–voltage characteristics of the Al/Au/n-Si nanodiode sensor; mass spectrometric data for the Al–water reaction on the nanodiode; SEM images of the Al surface (PDF)

### ■ AUTHOR INFORMATION

#### Corresponding Author

\*E-mail: [jeongypark@kaist.ac.kr](mailto:jeongypark@kaist.ac.kr).

#### ORCID

Jeong Young Park: 0000-0002-8132-3076

#### Present Address

#Department of Physics, Chalmers University of Technology, 412 96 Göteborg, Sweden (I.I.N.).

#### Notes

The authors declare no competing financial interest.

### ■ ACKNOWLEDGMENTS

This work was supported by the Institute for Basic Science (IBS) [IBS-R004].

### ■ REFERENCES

- (1) Luo, Z.; Castleman, A. W., Jr.; Khanna, S. N. Reactivity of Metal Clusters. *Chem. Rev.* **2016**, *116*, 14456–14492.
- (2) Li, F.; Sun, L.; Zhao, J.; Xu, F.; Zhou, H.-Y.; Zhang, Q.-M.; Huang, F.-L. Mechanisms of  $\text{H}_2$  Generation for Metal Doped  $\text{Al}_{10}\text{M}$  ( $\text{M} = \text{Mg}$  and  $\text{Bi}$ ) Clusters in Water. *Int. J. Hydrogen Energy* **2013**, *38*, 6930–6937.
- (3) Shimojo, F.; Ohmura, S.; Kalia, R. K.; Nakano, A.; Vashishta, P. Molecular Dynamics Simulations of Rapid Hydrogen Production from Water Using Aluminum Clusters as Catalysts. *Phys. Rev. Lett.* **2010**, *104*, 126102.
- (4) Dai, H. B.; Ma, G. L.; Xia, H. J.; Wang, P. Reaction of Aluminum with Alkaline Sodium Stannate Solution as a Controlled Source of Hydrogen. *Energy Environ. Sci.* **2011**, *4*, 2206–2212.
- (5) Shkolnikov, E. I.; Zhuk, A. Z.; Vlasin, M. S. Aluminum S Energy Carrier: Feasibility Analysis and Current Technologies Overview. *Renewable Sustainable Energy Rev.* **2011**, *15*, 4611–4623.
- (6) Huang, X.; Gao, T.; Pan, X.; Wei, D.; Lv, C.; Qin, L.; Huang, Y. A Review: Feasibility of Hydrogen Generation from the Reaction between Aluminum and Water for Fuel Cell Applications. *J. Power Sources* **2013**, *229*, 133–140.
- (7) Wang, H.; Leung, D. Y.; Leung, M. K. Energy Analysis of Hydrogen and Electricity Production from Aluminum-Based Processes. *Appl. Energy* **2012**, *90*, 100–105.

- (8) Wang, H. Z.; Leung, D. Y.; Leung, M. K. H.; Ni, M. A Review on Hydrogen Production Using Aluminum and Aluminum Alloys. *Renewable Sustainable Energy Rev.* **2009**, *13*, 845–853.
- (9) Shmelev, V.; Nikolaev, V.; Lee, J. H.; Yim, C. Hydrogen Production by Reaction of Aluminum with Water. *Int. J. Hydrogen Energy* **2016**, *41*, 16664–16673.
- (10) Rivero, U.; Álvarez-Barcia, S.; Flores, J. R. A Dynamical Model for the Generation of H<sub>2</sub> in Microhydrated Al Clusters. *Int. J. Hydrogen Energy* **2018**, *43*, 23285–23298.
- (11) Liu, Y.; Hua, Y.; Jiang, M.; Jiang, G.; Chen, J. Theoretical Study of the Geometries and Dissociation Energies of Molecular Water on Neutral Aluminum Clusters Al<sub>N</sub> (N = 2–25). *J. Chem. Phys.* **2012**, *136*, No. 084703.
- (12) Álvarez-Barcia, S.; Flores, J. R. Size, Adsorption Site, and Spin Effects in the Reaction of Al Clusters with Water Molecules: Al<sub>17</sub> and Al<sub>28</sub> as Examples. *J. Phys. Chem. A* **2012**, *116*, 8040–8050.
- (13) Pyun, S. I.; Moon, S. M. Corrosion Mechanism of Pure Aluminium in Aqueous Alkaline Solution. *J. Solid State Electrochem.* **2000**, *4*, 267–272.
- (14) Sze, S. M.; Ng, K. K. *Physics of Semiconductor Devices*; John Wiley & Sons, Inc., 10 April 2006.
- (15) Nedrygailov, I. I.; Karpov, E. G.; Hasselbrink, E.; Diesing, D. On the Significance of Thermoelectric and Thermionic Emission Currents Induced by Chemical Reactions Catalyzed on Nanofilm Metal-Semiconductor Heterostructures. *J. Vac. Sci. Technol., A* **2013**, *31*, No. 021101.
- (16) Nienhaus, H.; Bergh, H. S.; Gergen, B.; Majumdar, A.; Weinberg, W. H.; McFarland, E. W. Selective H Atom Sensors Using Ultrathin Ag Si Schottky Diodes. *Appl. Phys. Lett.* **1999**, *74*, 4046–4048.
- (17) Nienhaus, H.; Bergh, H. S.; Gergen, B.; Majumdar, A.; Weinberg, W. H.; McFarland, E. W. Direct Detection of Electron-Hole Pairs Generated by Chemical Reactions on Metal Surfaces. *Surf. Sci.* **2000**, *445*, 335–342.
- (18) Nienhaus, H.; Bergh, H. S.; Gergen, B.; Majumdar, A.; Weinberg, W. H.; McFarland, E. W. Electron-Hole Pair Creation at Ag and Cu Surfaces by Adsorption of Atomic Hydrogen and Deuterium. *Phys. Rev. Lett.* **1999**, *82*, 446–449.
- (19) Nienhaus, H.; Gergen, B.; Weinberg, W. H.; McFarland, E. W. Detection of Chemically Induced Hot Charge Carriers with Ultrathin Metal Film Schottky Contacts. *Surf. Sci.* **2002**, *514*, 172–181.
- (20) Park, J. Y.; Baker, L. R.; Somorjai, G. A. Role of Hot Electrons and Metal-Oxide Interfaces in Surface Chemistry and Catalytic Reactions. *Chem. Rev.* **2015**, *115*, 2781–2817.
- (21) Nienhaus, H. Electronic Excitations by Chemical Reactions on Metal Surfaces. *Surf. Sci. Rep.* **2002**, *45*, 1–78.
- (22) Nedrygailov, I. I.; Park, J. Y. The Nature of Hot Electrons Generated by Exothermic Catalytic Reactions. *Chem. Phys. Lett.* **2016**, *645*, 5–14.
- (23) Lee, H.; Nedrygailov, I. I.; Lee, C.; Somorjai, G. A.; Park, J. Y. Chemical Reaction-Induced Hot Electron Flows on Pt Colloid Nanoparticles under Hydrogen Oxidation: Impact of Nanoparticle Size. *Angew. Chem., Int. Ed.* **2015**, *54*, 2340–2344.
- (24) Lee, H.; Nedrygailov, I. I.; Lee, Y. K.; Lee, C.; Choi, H.; Choi, J. S.; Choi, C. G.; Park, J. Y. Graphene-Semiconductor Catalytic Nanodiodes for Quantitative Detection of Hot Electrons Induced by a Chemical Reaction. *Nano Lett.* **2016**, *16*, 1650–1656.
- (25) Kim, S. M.; Lee, H.; Park, J. Y. Charge Transport in Metal-Oxide Interfaces: Genesis and Detection of Hot Electron Flow and Its Role in Heterogeneous Catalysis. *Catal. Lett.* **2015**, *145*, 299–308.
- (26) Chen, H.-I.; Cheng, Y.-C.; Chang, C.-H.; Chen, W.-C.; Liu, I. P.; Lin, K.-W.; Liu, W.-C. Hydrogen Sensing Performance of a Pd Nanoparticle/Pd Film/Gan-Based Diode. *Sens. Actuators, B* **2017**, *247*, 514–519.
- (27) Rahbarpour, S.; Hosseini-Golgoob, S. M. Diode Type Ag–TiO<sub>2</sub> Hydrogen Sensors. *Sens. Actuators, B* **2013**, *187*, 262–266.
- (28) Ramgir, N. S.; Kaur, M.; Sharma, P. K.; Datta, N.; Kailasaganapathi, S.; Bhattacharya, S.; Debnath, A. K.; Aswal, D. K.; Gupta, S. K. Ethanol Sensing Properties of Pure and Au Modified ZnO Nanowires. *Sens. Actuators, B* **2013**, *187*, 313–318.
- (29) Nedrygailov, I. I.; Lee, C.; Moon, S. Y.; Lee, H.; Park, J. Y. Hot Electrons at Solid-Liquid Interfaces: A Large Chemoelectric Effect During the Catalytic Decomposition of Hydrogen Peroxide. *Angew. Chem., Int. Ed.* **2016**, *128*, 11017–11020.
- (30) Periasamy, V.; Rizan, N.; Al-Ta'ii, H. M. J.; Tan, Y. S.; Tajuddin, H. A.; Iwamoto, M. Measuring the Electronic Properties of DNA-Specific Schottky Diodes Towards Detecting and Identifying Basidiomycetes DNA. *Sci. Rep.* **2016**, *6*, 29879.
- (31) Talebi, S.; Daraghma, S.; Subramaniam, S. R. T.; Bhasu, S.; Periasamy, V. Exploring the Electronic Properties of Ribonucleic Acids Integrated within a Schottky-Like Junction. *J. Electron. Mater.* **2019**, *48*, 7114–7122.
- (32) Park, J. Y.; Kim, S. M.; Lee, H.; Nedrygailov, I. I. Hot-Electron-Mediated Surface Chemistry: Toward Electronic Control of Catalytic Activity. *Acc. Chem. Res.* **2015**, *48*, 2475–2483.
- (33) Nedrygailov, I. I.; Lee, C.; Moon, S. Y.; Lee, H.; Park, J. Y. Liquid-Phase Catalytic Reactor Combined with Measurement of Hot Electron Flux and Chemiluminescence. *Rev. Sci. Instrum.* **2016**, *87*, 114101.
- (34) Park, J. Y.; Lee, S. W.; Lee, C.; Lee, H. Strategies for Hot Electron-Mediated Catalytic Reactions: Catalytronics. *Catal. Lett.* **2017**, *147*, 1851–1860.
- (35) Gergen, B.; Nienhaus, H.; Weinberg, W. H.; McFarland, E. W. Chemically Induced Electronic Excitations at Metal Surfaces. *Science* **2001**, *294*, 2521–2523.
- (36) McFarland, E. W.; Weinberg, H. W.; Nienhaus, H.; Bergh, H. S.; Gergen, B.; Majumdar, A. Chemical Sensor Using Chemically Induced Electron-Hole Production at a Schottky Barrier. U.S. Patent US 7,057,213 B2, 2006.
- (37) Lee, S. H.; Nedrygailov, I. I.; Oh, S.; Park, J. Y. Hot Electron Flux at Solid-Liquid Interfaces Probed with Pt/Si Catalytic Nanodiodes: Effects of Ph During Decomposition of Hydrogen Peroxide. *Catal. Today* **2018**, *303*, 282–288.
- (38) Greber, T. Charge-Transfer Induced Particle Emission in Gas Surface Reactions. *Surf. Sci. Rep.* **1997**, *28*, 1–64.
- (39) Greber, T. Chemical Hole Diving. *Chem. Phys. Lett.* **1994**, *222*, 292–296.
- (40) Böttcher, A.; Grobecker, R.; Imbeck, R.; Morgante, A.; Ertl, G. Exoelectron Emission During Oxidation of Cs Films. *J. Chem. Phys.* **1991**, *95*, 3756–3766.
- (41) Böttcher, A.; Imbeck, R.; Morgante, A.; Ertl, G. Nonadiabatic Surface Reaction: Mechanism of Electron Emission in the Cs+O<sub>2</sub> System. *Phys. Rev. Lett.* **1990**, *65*, 2035–2037.
- (42) Kasemo, B. Photon Emission During Chemisorption of Oxygen on Al and Mg Surface. *Phys. Rev. Lett.* **1974**, *32*, 1114–1117.
- (43) Kasemo, B.; Törnqvist, E.; Walldén, L. Metal-Gas Reactions Studied by Surface Chemiluminescence. *Mater. Sci. Eng.* **1980**, *42*, 23–29.
- (44) Kasemo, B.; Walldén, L. Photon and Electron Emission During Halogen Adsorption on Sodium. *Surf. Sci.* **1975**, *53*, 393–407.
- (45) Liu, X.; Cuenya, B. R.; McFarland, E. W. A Mis Device Structure for Detection of Chemically Induced Charge Carriers. *Sens. Actuators, B* **2004**, *99*, 556–561.
- (46) Hagemann, U.; Timmer, M.; Krix, D.; Kratzer, P.; Nienhaus, H. Electronic Excitations in Magnesium Epitaxy: Experiment and Theory. *Phys. Rev. B* **2010**, *82*, 155420.
- (47) Palm, H.; Arbes, M.; Schulz, M. Fluctuations of the Au-Si(100) Schottky-Barrier Height. *Phys. Rev. Lett.* **1993**, *71*, 2224–2227.
- (48) Lin, Y.-J.; Huang, B.-C.; Lien, Y.-C.; Lee, C.-T.; Tsai, C.-L.; Chang, H.-C. Capacitance–Voltage and Current–Voltage Characteristics of Au Schottky Contact on N-Type Si with a Conducting Polymer. *J. Phys. D: Appl. Phys.* **2009**, *42*, 165104.